Publishing Excellence Inspiring Progress
ARISTON PUBLICATIONS
MatSci Express
ISSN: 2997-8440 www.aristonpubs.com/matsci-express https://doi.org/10.69626/mse.2024.0253

RESEARCH ARTICLE

Development and Modelling of a Photonic Crystal Fiber Sensor for Detecting Harmful Chemicals in Polycarbonate Plastics

Pratishtha Pandey [1], Sapana Yadav [1], D. K. Dwivedi [1,*], Pooja Lohia [2]

ABSTRACT: This study presents the development and modeling of a photonic crystal fiber (PCF) sensor designed for detecting harmful chemicals in polycarbonate plastics. The sensor features a wheel-shaped PCF structure with a floral pattern in the initial cladding layer. The focus is on two significant chemical compounds commonly found in plastics, bisphenol A (BPA) and bisphenol S (BPS). The individual sensitivities of the sensor to these compounds are measured, achieving relative sensitivities of 90.716% for BPS and 84.688% for BPA. The effective refractive indices for BPS and BPA are found to be 1.499 and 1.550, respectively. Additionally, the study analyzes confinement loss and nonlinearity of the proposed structure when exposed to these compounds, demonstrating low confinement loss and high nonlinearity, which are desirable attributes for sensing applications. The octagonal floral structure of the PCF sensor shows potential for a variety of applications, including chemical and biochemical sensing and nonlinear optics. The propagation characteristics and performance of the wheel-shaped hollow-core PCF have been thoroughly analyzed within the wavelength range of 1.5 µm to 2.5 µm. The sensor, utilizing silica as the background material, exhibits high sensitivity and low confinement loss. The analysis indicates that increasing the number of air holes in the cladding and enlarging the core size, where electromagnetic waves interact with the analyte, can further enhance sensitivity and detection accuracy with minimal losses. The PCF sensor offers real-time, label-free detection of chemical compounds with a high birefringence of -9.594×10^{-5}, a highest refractive index (RI) of 1.550, and an effective area of 4.373×10^{-12} m^2 for BPS at 1.2 µm. The proposed method yields negligible confinement loss, making it suitable for applications in optical fiber sensing, optical waveguides, and various photonic devices.

Keywords: Photonic crystal fiber, Polycarbonate plastic, Relative sensitivity, Bisphenol A, Bisphenol S, Nonlinearity

Received: 05 April 2024; Revised: 29 May 2024; Accepted: 13 July 2024; Published Online: 22 July, 2024

1. INTRODUCTION

In today's technology, photonic crystal fibers (PCFs) sensors shine with their advancements in sensing applications when compared to traditional optical fibers [1]. Researchers have explored into the distinctive qualities of PCFs, such as their cost-effectiveness, durability, high birefringence, compact size, and minimal signal loss [2]. Furthermore, PCFs exhibit remarkable operational capabilities in demanding environments, including intense electromagnetic fields, high voltages, chemically harsh conditions, noisy surroundings, and high-temperature settings. Essentially, PCFs constitute a class of optical fibers characterized by a periodic arrangement of low-index and high-index airholes throughout their length. There are primarily two mechanisms for guiding light in photonic crystal fiber: in solid-core PCFs, light is confined within the high refractive index region via modified total internal reflection (MTIR) mechanism, while in PCFs with a low-index core material surrounded by high-index cladding material, light confinement occurs through the photonic band gap effect [3]. PCFs enable precise manipulation of fiber propagation characteristics by

[1] Photonics and Photovoltaic Research Lab (PPRL), Department of Physics and Material Science, Madan Mohan Malaviya University of Technology, Gorakhpur-273010, India.
[2] Department of Electronics and Communication Engineering, Madan Mohan Malaviya University of Technology, Gorakhpur-273010, India

* Author to whom correspondence should be addressed: todkdwivedi@gmail.com (D. K. Dwivedi)

adjusting the shape, size, and positions of air holes. By modifying these geometric parameters, a broad range of guiding properties can be attained in PCFs [4]. Traditional optical fibers have inherent limitations stemming from their structural composition, but these restrictions are effectively mitigated by Photonic Crystal Fibers (PCF) due to their distinctive design. Within PCF, a consistent layout of microstructure apertures influences the behaviour of photons. Light is guided in PCF through modified total internal reflection or photonic band gap (PBG) guidance [5]. Typically, PCF background material comprises pure silica, which maintains a constant Refractive Index (RI) of 1.44 along the waveguide, while air holes spanning the fiber's length establish a low-index region. Optical fiber sensors are garnering significant interest in modern science and manufacturing technology owing to their versatility, high sensitivity, adaptable design, compact size, stability, multiplexing capabilities, and remote sensing potential. Several research investigations have immersed into techniques to improve the propagation properties of PCF [6]. The escalating concern revolves around the exposure of most individuals to industrial chemicals. Among these, bisphenol A (BPA) stands out as one of the most harmful substances, commonly utilized in the production of polycarbonate plastics and epoxy resins [7]. They are used in making water bottles, food and beverage containers, baby bottles, kitchenware, baking utensils, orthodontic products, eyewear, automotive components, optical discs, medical tools, and tubing, among others. These products can leach BPA, an endocrine-disrupting compound capable of interfering with estrogen hormones, particularly posing risks to females and children. Its detrimental impacts encompass infertility, diabetes, obesity, behavioural alterations, chemotherapy resistance, and potential links to breast and prostate cancer [8].

Several researchers have proposed various designs aimed at detecting harmful chemicals present in plastic components. Jibon et al. highlighted the hazards associated with BPA, and BPS, suggesting a sensor based on PCF (Photonic Crystal Fiber) to identify these substances which achieved relative sensitivities of 96.5% for BPA, and 97.6% for BPS at the optimal wavelength [9]. On the other hand, Niger and Hasin proposed a different PCF design for the same purpose, utilizing Zeonex material. Their sensor architecture features a large square core hole intended for analyte infiltration, measuring 500 µm in length. This PCF sensor, achieved relative sensitivities exceeding 94% for all tested analytes, specifically 95.8% for BPA, and 96.1% for BPS [10].

Previous intricate PCF designs have shown reasonable relative sensitivity in detecting chemicals like BPA, DEHP, and BPS within plastic materials. However, these earlier designs often required specific raw materials, reducing cost-effectiveness for large-scale applications. Additionally, it has become evident that highly sensitive sensing can be achieved with smaller micro structured designs. Considering these aspects, this study introduces a novel PCF design characterized by simplicity, cost-effectiveness, and exceptional sensing capabilities. Operating in the visible to infrared wavelength range of 1.5–2.5 µm, the proposed design features a single circular core hole complemented by wheel shaped air holes layers of circular cladding air holes arranged in lattice. This innovative structural arrangement results in significantly improved optical and sensing performance, with relative sensitivities consistently exceeding 92%, and confinement losses remaining impressively low, ranging from -9.564×10^{-6} dB/cm for all tested analytes.

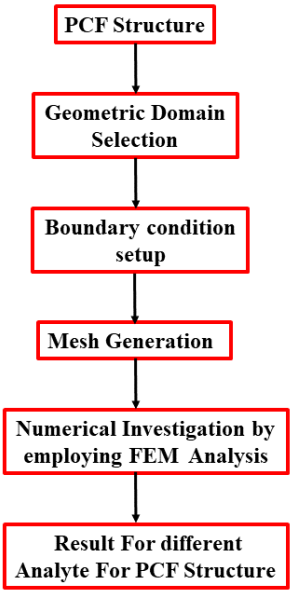

Fig. 1. Flow chart for FEM based simulation.

2. DESIGN CONSIDERATION AND PERFORMANCE PARAMETER

2.1. Proposed Design

Figure 1 depicts the proposed PCF-based chemical sensor designed to ensure high fabrication feasibility. The sensor comprises a single hollow core at the centre surrounded by a primary layer of eight elliptical airholes around the core. The central core contains samples of two synthesized polycarbonate substances (BPA and BPS) for detection purposes. The suggested PCF operates within the wavelength range of 1.5 µm to 2.5µm. Simulation of the proposed design has been conducted using the finite element method with COMSOL Multiphysics v6.1a software due to its superior computational efficiency. The proposed design is illustrated in Figure 2 (a), employing Perfectly Matched Layers (PML) with a thickness of 10% of the maximum fiber width and a core diameter of dc. The first layer of circular representation features circles of diameter d1, while the second layer has circles of diameter d2. The strut size (distance between two closest airholes) is denoted by V. Table 1 presents the values of optimal design parameters.

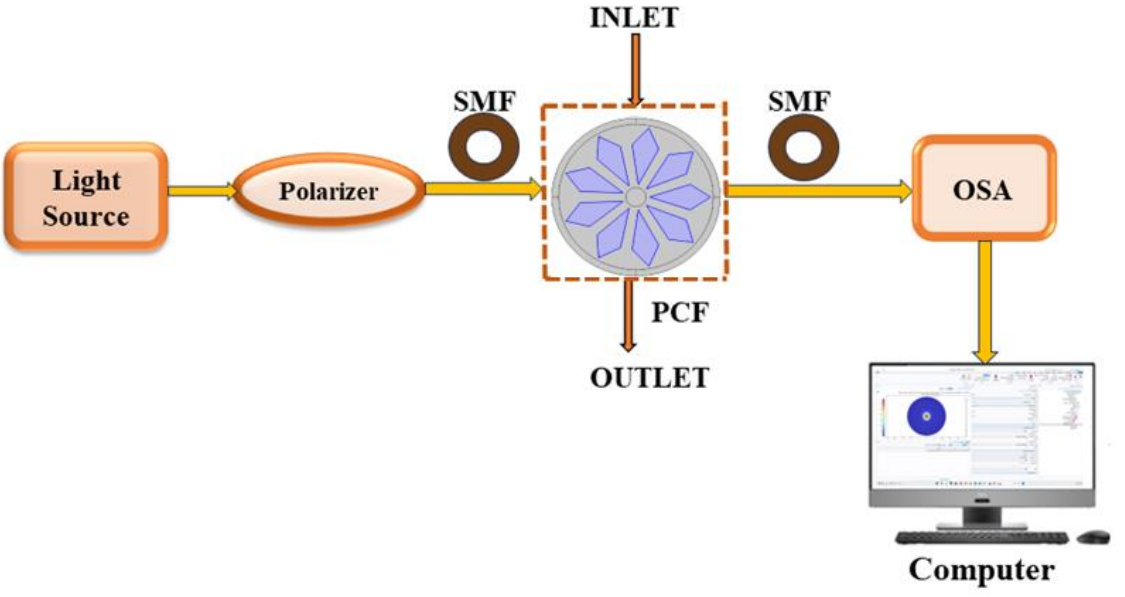

Fig. 2. Schematic illustration of experimental setup.

Physics-controlled meshing and finer element size have been chosen for the meshing of the proposed design. Figure 2(b) displays the computational meshing domain, comprising 48 vertex elements, 399 boundary elements, and 1912 total elements The background material employed in sensor design is pure silica, known for its exceptional optical properties, including high optical transparency, superior resistance to acidity, insensitivity to humidity, and low material dispersion [11]. The refractive index of fused silica is determined using the Sellemeier equation [12].

$$n(\lambda)^2 = 1 + \frac{0.696\lambda^2}{\lambda^2 - 0.00047} + \frac{0.408\lambda^2}{\lambda^2 - 0.14} + \frac{0.897\lambda^2}{\lambda^2 - 97.934} \quad (1)$$

The Table 1 depicts the refractive index of different plastic samples analyzed in this study. The refractive index is a crucial parameter in understanding how light interacts with the material, which directly affects the performance of the photonic crystal fiber sensor. The refractive indices listed in Table 1 highlight the differences in optical properties between BPA and BPS, two common plasticizers.

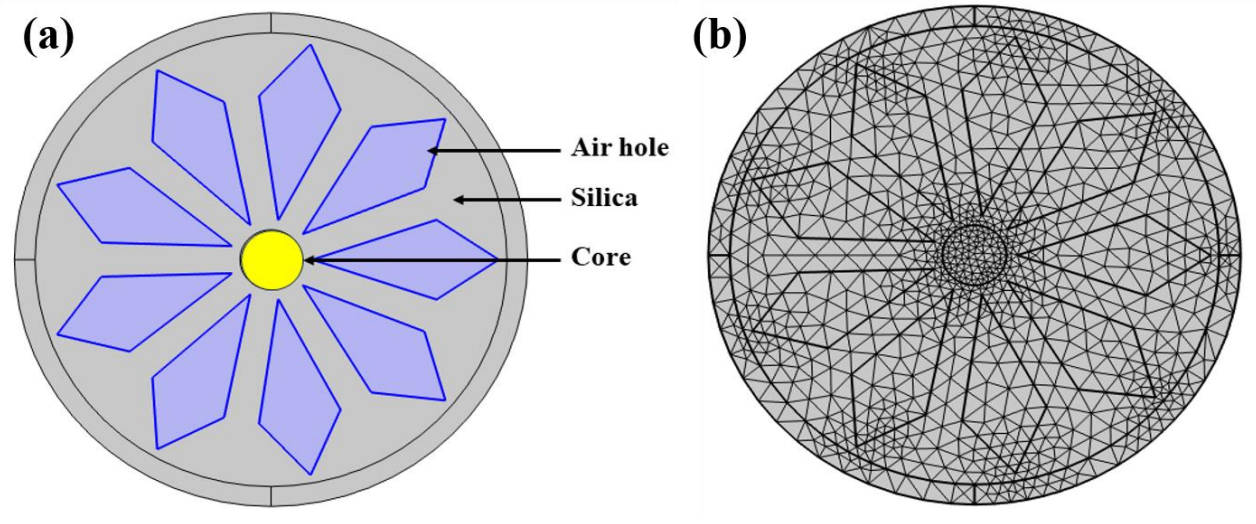

Fig. 3. (a) Schematic Diagram of hollow core PCF sensor, and (b) Finer meshing output.

Bisphenol A (BPA) has a refractive index of 1.585, while Bisphenol S (BPS) has a higher refractive index of 1.645. These values indicate that BPS has a greater ability to bend light compared to BPA. The differences in refractive index are significant for the design and optimization of the PCF sensor. A higher refractive index, such as that of BPS, implies stronger light confinement within the core of the fiber, potentially enhancing the sensitivity of the sensor to detect this chemical. Conversely, the slightly lower refractive index of BPA suggests that the sensor might need additional optimization to achieve similar sensitivity levels.

2.2. Fabrication feasibility

Ensuring the feasibility of fabrication emerges as a pivotal factor in determining the usability of sensors. Various methods are available for producing Photonic Crystal Fibers (PCF) with microstructural waveguides, including stack and draw, sol-gel [13], extrusion [14], drilling [15], preform moulding, and 3D printing [15]. Sol-gel and drilling methods are commonly employed for constructing structures with circular airholes, while stack and draw are effective for circular airhole designs. For asymmetric airholes like elliptical, rectangular, or square shapes, 3D printing, and extrusion methods are extensively utilized and prove to be the most suitable techniques. The selected structure aims to tightly guide light within the PCF core for the detection of harmful chemicals with relatively high refractive index (n_{eff}).

3. METHODOLOGY AND PERFORMANCE PARAMETER

The sensor's performance can be evaluated based on specific sensing properties such as confinement loss, relative sensitivity, effective area, power ratio, propagation constant, and relative sensitivity, which are among the most critical characteristics. Typically, sensing involves comparing the effective refractive index (neff). The proposed fiber sensor, operating in the micrometre range, demonstrates a wide effective area with relatively low confinement and higher relative sensitivity. In sensing applications, it is imperative that light is both propagated and confined within the core region. The velocity of light is affected by the refractive index of the medium.

3.1. Relative sensitivity

The relative sensitivity correlates directly with the power within the core region, serving as an indicator of both the presence and quantity of the analyte within the fiber's core. This parameter is determined using a modified Beer-Lambert law equation:

$$Rs = \left(\frac{n_a}{n_{eff}}\right) P \quad (2)$$

Here, n_a signifies the refractive index of drug analyte, n_{eff} represents the effective refractive index and "P" stands for the power factor ratio [16].

Power factor ratio (P) quantifies the amount of light power propagated through the present sensing analyte in the core and is calculated by poynting theorem.

$$P = \frac{\text{sample}\int \text{Re}(E_xH_y - H_xE_y,)d_xd_y}{\text{total}\int \text{Re}(E_xH_y - H_xE_y)d_xd_y} \times 100\% \quad (3)$$

In this expression, H_x, E_x denotes diagonal magnetic field and electric field respectively, and H_y, E_y represents longitudinal magnetic field and electric field respectively, for both *x* and *y* polarizations.

3.2. Effective Area

The effective area (EA) signifies the coverage area within the core where analyte sensing is exceptionally effective and also reflects the quality of light propagating through the core. The intensities of light that propagate through the core interact with the analyte present in the core. A lower value of EA is essential to improve sensor performance [3]:

$$EA = \frac{(\int|E^2|d_xd_y)^2}{\int|E^4|d_xd_y} \quad (4)$$

3.3. Effective Refractive Index

The effective refractive index (n_{eff}) carries a similar significance in describing the propagation of light within a waveguide. The n_{eff} of the cladding region is determined based on the propagation constant of the lowest mode order capable of propagating within the finite cladding media, as expressed in the equation [17]:

$$n_{eff} = \frac{\beta}{k_0} \quad (5)$$

Here, $k_0=2\pi / \lambda$; λ is operating wavelength of light, β is propagation constant

3.4. Nonlinearity

The nonlinearity of a PCF is contingent on both the analyte concentration within the core volume and the asymmetry of the fiber mode, which can be manipulated by adjusting the size and position of air holes in the cladding region. Additionally, nonlinearity is influenced by the effective area (EA). The nonlinearity coefficient (γ) demonstrates an inverse correlation with the effective area (EA). A greater effective mode area is associated with reduced nonlinearity [3].

$$\gamma = (\frac{2\pi f}{c})(\frac{n_2}{EA}) \quad (6)$$

3.5. Propagation constant

The propagation constant of a mode within fiber, predict the way the amplitude and phase of that light at a certain frequency change along the direction of propagation z. The propagation constant is dependent on the operating wavelength of the light. The variation in wavelength dependence of its imaginary part determines the group delay of waveguide [3]. Mathematical expression for propagation constant is given as:

$$\beta = (\frac{2\pi f}{c})\text{Imag}[n_{eff}] \quad (7)$$

3.6. Confinement loss

In the process of optical transmission, optical fibers encounter confinement loss, representing the ability to confine light within the core region. The presence of airholes in the cladding leads to light leakage into the cladding area. Aligning the airholes properly in both the core and cladding areas reduces confinement loss (CL). A lower CL value positively impacts the sensitivity and efficiency of a PCF-based biosensor. The numerical assessment of confinement loss is provided to quantify this phenomenon [18]:

$$CL = (\frac{4\pi f}{c})\text{Imag}[n_{eff}] \quad (8)$$

4. RESULTS AND DISCUSSION

The numerical analysis of the PCF sensor's performance focuses on three chemical materials: BPA and BPS In evaluating the efficacy of the designed PCF sensor, various optical properties such as effective mode index, power factor, relative sensitivity, effective area, effective refractive index, and confinement loss are examined within the spectral range of 1.5–2.5 μm.

Figure 4 showcases the propagation of light through the photonic crystal fiber (PCF) sensor when exposed to bisphenol A (BPA) and bisphenol S (BPS) in both x- and y-polarizations. The figure highlights regions with maximum light confinement using a yellow-red color scheme. These regions indicate where the light is most effectively confined within the core of the sensor, which is crucial for enhancing sensor efficiency and sensitivity. The strong confinement shown in these regions ensures that the light interacts more effectively with the analytes, thereby improving the sensor's ability to detect the presence of harmful chemicals in the polycarbonate plastics. The observed high confinement for both polarizations underscores the sensor's robustness and effectiveness in various operational conditions.

Figure 5 depicts the variation of the effective refractive index with the operating wavelength for the proposed PCF sensor structures. The graph shows that the effective refractive index for both BPA and BPS decreases slightly as the wavelength increases. This trend indicates that the propagation of electromagnetic (EM) waves is more pronounced in the cladding area, particularly for BPS, which has a higher effective refractive index of 1.550 compared to 1.499 for BPA.

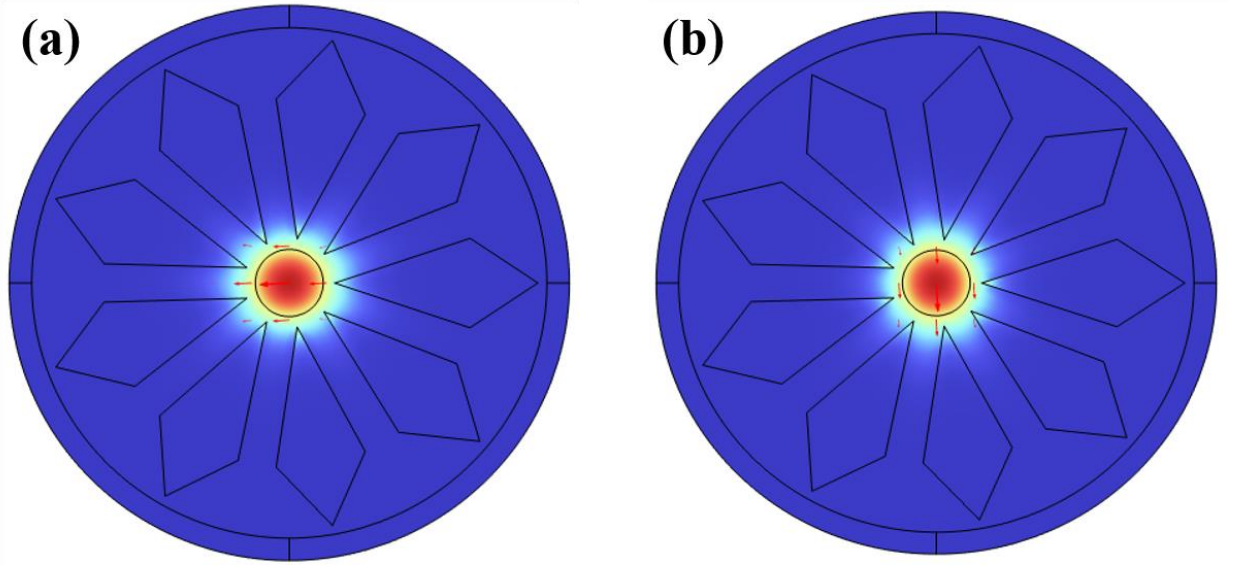

Fig. 4. Field distribution for (a), x- polarization mode and (b) y polarization mode of light for sensor.

This difference suggests that BPS interacts more strongly with the PCF sensor, enhancing its detection capabilities for this specific compound. The gradual decrease in the refractive index with increasing wavelength is typical and reflects the wavelength-dependent optical properties of the sensor.

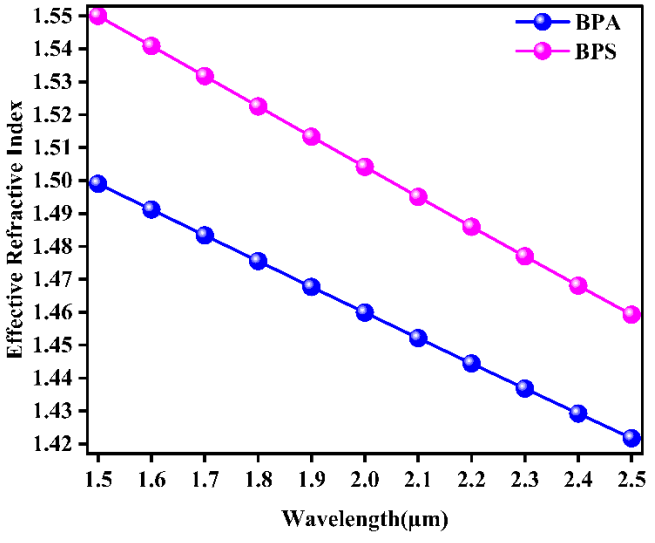

Fig. 5. Variation of Effective-RI with wavelength for proposed sensor design.

Figure 6 illustrates the effective area of the PCF sensor's core design across a wavelength range of 1.5 µm to 2.5 µm. The graphs reveal an increasing trend in the effective area with incremental wavelength, which can be attributed to the compactness of the transverse electric field within the core region. For the proposed sensor design, the effective area is larger for BPA, measuring 5.387×10^{-12} m², compared to 4.373×10^{-12} m² for BPS. This increasing effective area with wavelength suggests that the light's interaction with the core becomes less confined, which may influence the sensor's sensitivity and detection limits. The larger effective area for BPA indicates that it requires more space for effective light-matter interaction compared to BPS, which is more efficiently confined within the core.

Figure 7 presents graphs illustrating the relative sensitivity of two distinct PCF sensor designs across various analytes, specifically focusing on BPA and BPS. Relative sensitivity, a crucial parameter for PCF sensors, reflects how well the sensor detects changes in the refractive index of the surrounding medium. Both graphs show peak sensitivity values at 1.5 µm, indicating optimal light confinement within the core region at this wavelength. As the wavelength increases, relative sensitivity diminishes for all analytes, which is attributed to light leakage into the cladding region. This leakage limits effective light confinement to the far infrared region, from 1.5 µm to 2.5 µm. For the sensor design, BPS shows the highest relative sensitivity at 90.716%, followed by BPA at 84.688%. This indicates that the sensor is more efficient at detecting BPS compared to BPA.

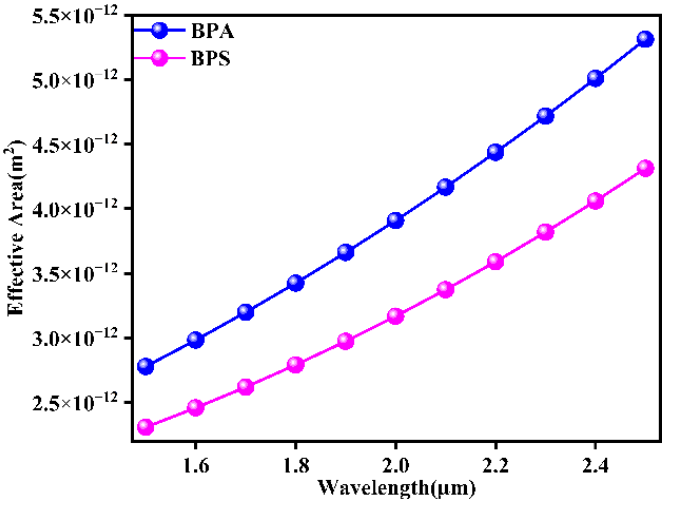

Fig. 6. Variation of Effective Area with wavelength for proposed sensor.

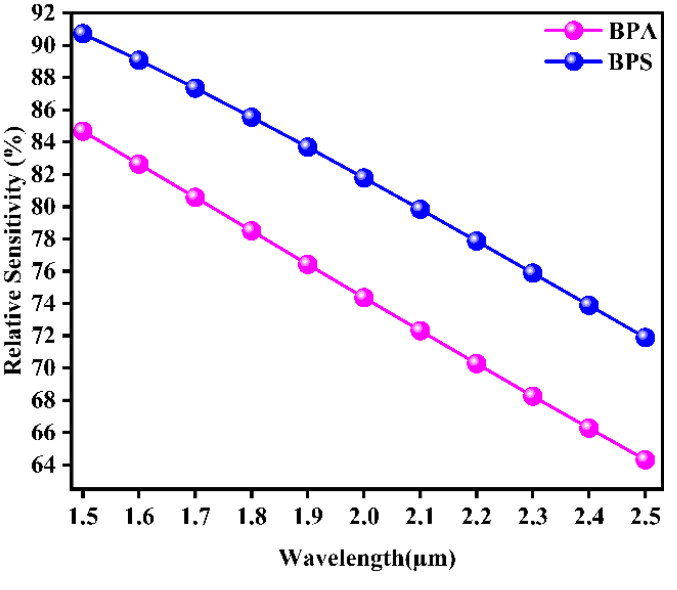

Fig. 7. Variation of Relative Sensitivity with Wavelength for Sensor Design.

Figure 8 depicts the nonlinearity of the sensor design, demonstrating a decrease in nonlinearity as the wavelength increases from 1.5 µm to 2.5 µm. Nonlinearity in PCF sensors is influenced by factors such as light leakage and effective area. The graph shows that the highest nonlinearity value is obtained for BPS at 58.220 $W^{-1}Km^{-1}$, followed by BPA at 48.670 $W^{-1}Km^{-1}$. This high nonlinearity is due to slight light leakage into the cladding, which is more pronounced at shorter wavelengths due to the larger effective area and smaller effective refractive index (neff). As the wavelength

increases, nonlinearity decreases, indicating reduced interaction between the light and the core material.

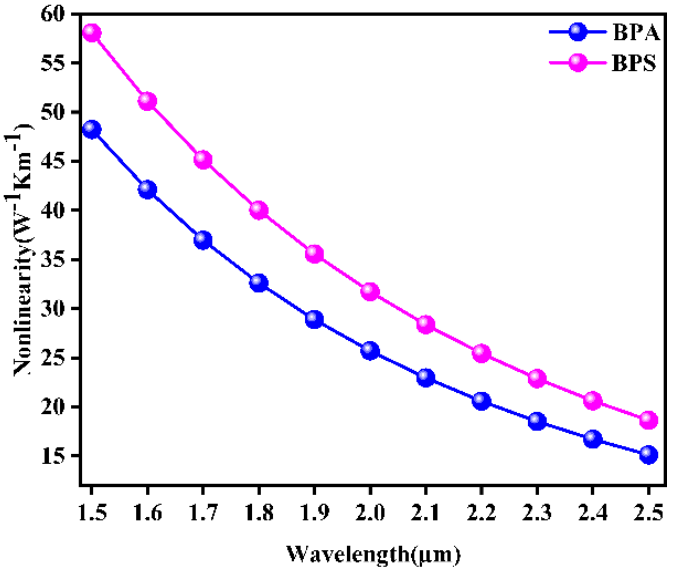

Fig. 8. Variation of Nonlinearity with Wavelength for Sensor Design.

Figure 9 illustrates the confinement loss (CL) curves for the PCF design when exposed to various analytes. Confinement loss measures how much light is lost from the core into the cladding, and it is a critical factor for sensor performance. The graph shows that BPA has the lowest CL value, followed by BPS, indicating superior light confinement within the core region. The minimum CL values are -9.5×10^{-6} dB/cm for BPA and 0 dB/cm for BPS. These low values suggest that the sensor design is highly effective in minimizing light loss, which is essential for accurate and sensitive detection.

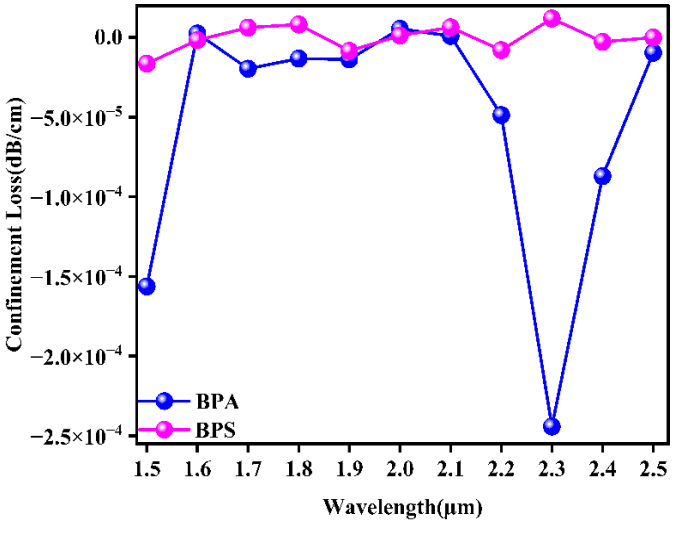

Fig. 9. Variation of Confinement Loss with Wavelength for PCF Design.

Figure 10 reports the propagation constant values for BPA and BPS in the given sensor design. The propagation constant, which is half of the obtained confinement loss value, indicates how efficiently light propagates through the fiber. The graph shows that the propagation constant values are 0 and -4.8×10^{-6} for BPA and BPS, respectively. These values are almost negligible within the specific wavelength region, suggesting minimal attenuation and efficient light propagation through the fiber, which is crucial for high-performance sensing applications.

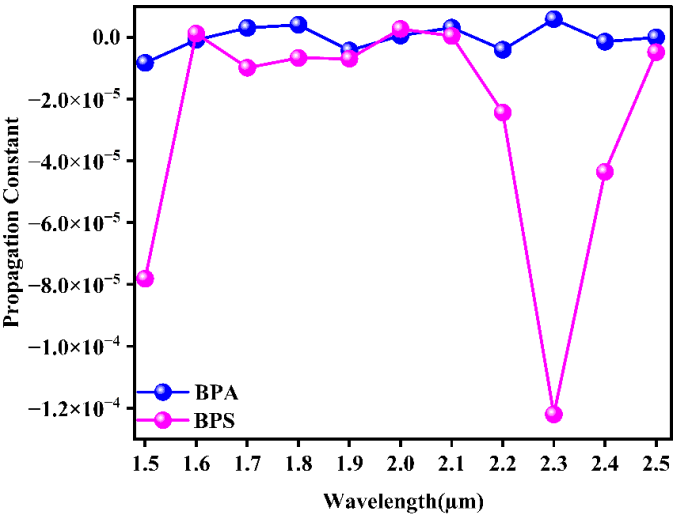

Fig. 10. Variation of Propagation Constant with Wavelength for PCF Design.

Table 2. Values Acquired for Various Parameters for the Proposed Sensor.

Parameter	BPA	BPS
Relative sensitivity	84.688%	90.716%
Effective refractive index	1.499	1.550
Effective area(m^2)	2.788× 10^{-12}	2.316 × 10^{-12}
Confinement loss (dB/cm)	0	-9.564×10^{-6}
Nonlinearity	48.220	58.070
Propagation constant	0	-4.780×10^{-6}

Table 2 summarizes the values for key parameters of the proposed sensor when exposed to BPA and BPS. The relative sensitivity is highest for BPS at 90.716%, compared to 84.688% for BPA. The effective refractive index is 1.499 for BPA and 1.550 for BPS, indicating a stronger interaction with the fiber core for BPS. The effective area is 2.788×10^{-12} m² for BPA and 2.316×10^{-12} m² for BPS, reflecting the area over which the light interacts with the analytes. The confinement loss is 0 dB/cm for BPA and -9.564×10^{-6} dB/cm for BPS, indicating very low light loss for both analytes. Nonlinearity

values are 48.220 $W^{-1}Km^{-1}$ for BPA and 58.070 $W^{-1}Km^{-1}$ for BPS, and the propagation constant values are 0 for BPA and -4.780×10^{-6} for BPS, indicating efficient light propagation and minimal attenuation. This table highlights the superior performance of the proposed sensor in detecting BPS compared to BPA.

4. CONCLUSION

In this study, we analyzed the propagation characteristics and performance of a wheel-shaped hollow-core photonic crystal fiber (HC-PCF) sensor for detecting harmful chemicals in polycarbonate plastics, focusing on bisphenol A (BPA) and bisphenol S (BPS). The analysis covered a wavelength range of 1.5 µm to 2.5 µm, utilizing silica as the background material. The proposed sensor exhibited high sensitivity and low confinement loss, essential for effective chemical detection. By optimizing the sensor design, including increasing the number of air holes in the cladding and enlarging the core size, we achieved better confinement of electromagnetic waves within the core, enhancing sensitivity and detection accuracy for real-time and label-free detection. The sensor achieved a high birefringence of -9.594×10^{-5} and an effective refractive index (RI) of 1.550 for BPS at a wavelength of 1.2 µm. The effective area for BPS was 4.373×10^{-12} m^2, indicating the sensor's capability to detect minor changes in the presence of analyte, making it effective for environmental monitoring and safety applications. Additionally, the sensor exhibited negligible confinement loss, crucial for maintaining signal integrity over long distances, suitable for optical fiber sensing, optical waveguides, and other photonic devices. High relative sensitivity values were observed for BPS (90.716%) and BPA (84.688%), validating the sensor's efficacy. The nonlinearity values decreased with increasing wavelength, and the minimal propagation constant values highlighted the sensor's robust performance across the studied wavelength range. The proposed wheel-shaped HC-PCF sensor offers a viable and efficient solution for detecting harmful chemicals in polycarbonate plastics. Its design provides significant advantages in sensitivity, accuracy, and low confinement loss, making it a promising tool for various applications in chemical and biochemical sensing, nonlinear optics, and environmental monitoring. Future work could explore further optimizations and potential applications, leveraging the sensor's capabilities for broader industrial and research uses.

CONFLICT OF INTEREST

The authors declare that there is no conflict of interests.

REFERENCES

[1] Pinto, A.M. and Lopez-Amo, M., **2012.** Photonic crystal fibers for sensing applications. *Journal of Sensors*, *2012*(1), p.598178.

[2] Chaudhary, V.S., Kumar, D., Pandey, B.P. and Kumar, S., **2022.** Advances in photonic crystal fiber-based sensor for detection of physical and biochemical parameters—A review. *IEEE Sensors Journal*, *23*(2), pp.1012-1023.

[3] Kumar, P., Kumar, V. and Roy, J.S., **2019.** Design of quad core photonic crystal fibers with flattened zero dispersion. *AEU-International Journal of Electronics and Communications*, *98*, pp.265-272.

[4] Prajapati, Y.K., Kumar, R. and Singh, V., **2019.** Design of a photonic crystal Fiber for dispersion compensation and sensing applications using modified air holes of the cladding. *Brazilian Journal of Physics*, *49*, pp.745-751.

[5] Sardar, M.R., Faisal, M. and Ahmed, K., **2021.** Simple hollow core photonic crystal fiber for monitoring carbon dioxide gas with very high accuracy. *Sensing and Bio-Sensing Research*, *31*, p.100401.

[6] Habib, M.A., Anower, M.S., Abdulrazak, L.F. and Reza, M.S., **2019.** Hollow core photonic crystal fiber for chemical identification in terahertz regime. *Optical Fiber Technology*, *52*, p.101933.

[7] Rather, J.A. and De Wael, K., **2013.** Fullerene-C60 sensor for ultra-high sensitive detection of bisphenol-A and its treatment by green technology. *Sensors and Actuators B: Chemical*, *176*, pp.110-117.

[8] Dong, X., Qi, X., Liu, N., Yang, Y. and Piao, Y., **2017.** Direct electrochemical detection of bisphenol A using a highly conductive graphite nanoparticle film electrode. *Sensors*, *17*(4), p.836.

[9] Jibon, R.H., Ahmed, M. and Hasan, M.K., **2021.** Identification of detrimental chemicals of plastic products using PCF in the THz regime. *Measurement: Sensors*, *17*, p.100056.

[10] Maidi, A.M.I., Salam, R., Kalam, M.A. and Begum, F., **2024.** Design and simulation of photonic crystal fibre sensor for harmful chemicals detection in polycarbonate plastics. *Optical and Quantum Electronics*, *56*(1), p.31.

[11] Anthony, J., Leonhardt, R., Argyros, A. and Large, M.C., **2011.** Characterization of a microstructured Zeonex terahertz fiber. *Journal of the Optical Society of America B*, *28*(5), pp.1013-1018.

[12] Ghosh, G., **1995.** Sellmeier coefficients and chromatic dispersions for some tellurite glasses. *Journal of the*

American Ceramic Society, *78*(10), pp.2828-2830.

[13] Hasan, M.R., Islam, M.A. and Rifat, A.A., **2016.** A single mode porous-core square lattice photonic crystal fiber for THz wave propagation. *Journal of the European Optical Society*, *12*, pp.1-8.

[14] Ghazanfari, A., Li, W., Leu, M.C. and Hilmas, G.E., **2017.** A novel freeform extrusion fabrication process for producing solid ceramic components with uniform layered radiation drying. *Additive Manufacturing*, *15*, pp.102-112.

[15] Zhang, P., Zhang, J., Yang, P., Dai, S., Wang, X. and Zhang, W., **2015.** Fabrication of chalcogenide glass photonic crystal fibers with mechanical drilling. *Optical Fiber Technology*, *26*, pp.176-179.

[16] Hossain, M.S., Sen, S. and Hossain, M.M., **2020**. Design of a chemical sensing circular photonic crystal fiber with high relative sensitivity and low confinement loss for terahertz (THz) regime. *Optik*, *222*, p.165359.

[17] Arif, M.F.H., Hossain, M.M., Islam, N. and Khaled, S.M., **2019.** A nonlinear photonic crystal fiber for liquid sensing application with high birefringence and low confinement loss. *Sensing and Bio-Sensing Research*, *22*, p.100252.

[18] Saitoh, K. and Koshiba, M., **2003.** Leakage loss and group velocity dispersion in air-core photonic bandgap fibers. *Optics Express*, *11*(23), pp.3100-3109.